J|A|C|S
ARTICLES
Published on Web 01/14/2006

Synthesis and Photoelectron Spectroscopic Studies of $N(CH_2CH_2NMe)_3P{=}E$ (E = O, S, NH, CH_2)

Tamás Kárpáti,[†] Tamás Veszprémi,[†] Natesan Thirupathi,[‡] Xiaodong Liu,[‡] Zhigang Wang,[‡] Arkady Ellern,[‡] László Nyulászi,*[,†] and John G. Verkade*[,‡]

Contribution form the Department of Inorganic Chemistry, Budapest University of Technology and Economics, H-1521 Budapest, Hungary, Department of Chemistry, Iowa State University, Ames, Iowa 50011

Received July 15, 2005; E-mail: nyulaszi@mail.bme.hu

Abstract: The synthesis and the crystal and molecular structure of $N(CH_2CH_2NMe)_3P{=}CH_2$ is reported. The $P-N_{ax}$ distance is rather long in $N(CH_2CH_2NMe)_3P{=}CH_2$. The ylide $N(CH_2CH_2NMe)_3P{=}CH_2$ proved to be a stronger proton acceptor than proazaphosphatrane $N(CH_2CH_2NMe)_3P$, since it was shown to deprotonate $N(CH_2CH_2NMe)_3PH^+$. The extremely strong basicity of the ylide is in accordance with its low ionization energy (6.3 eV), which is the lowest in the presently investigated series $N(CH_2CH_2NMe)_3P{=}E$ (E: CH_2, NH, lone pair, O and S), and to the best of our knowledge it is the smallest value observed for a non-conjugated phosphorus ylide. Computations reveal the existence of two bond strech isomers, and the stabilization of the phosphorus centered cation by electron donation from the equatorial and the axial nitrogens. Similar stabilizing effects operate in the case of protonation of E. A fine balance of these different interactions determines the $P-N_{ax}$ distance, which is thus very sensitive to the level of the theory applied. According to the quantum mechanical calculations, methyl substitution at the equatorial nitrogens flattens the pyramidality of this atom, increasing its electron donor capability. As a consequence, the PN_{ax} distance in the short-transannular bonded protonated systems and the radical cations is longer by about 0.5 Å in the $N_{eq}(Me)$ than in the $N_{eq}(H)$ systems. Accordingly, isodesmic reaction energies show that a stabilization of about 25 and 10 kcal/mol is attributable to the formation of the transannular bond in case of $N_{eq}(H)$ and the experimentally realizable $N_{eq}(Me)$ species, respectively.

Introduction

Tris(dialkylamino)phosphine ylides **1**[1] and **2**−**4**[2] are useful as strong neutral Bronsted bases,[2] as reactants in the Wittig reaction,[1b,2] and in the case of **3**, as a valuable starting material for the preparation of titanium-substituted ylides used as precursors for the preparation of allenes.[3] The structural and bonding features of **1**[1] and **2**−**4** are also of interest.[4] In 1998 we reported the in situ preparation of **1** from $\mathbf{1H}^+_{(C)}$[5] and sodium bis(trimethylsilyl)amide.[1] Compound **1** was subsequently structurally characterized by X-ray crystallography and utilized in our laboratories for the conversion of aldehydes to alkenes in high yield with quantitative *E* selectivity via the Wittig reaction.[1b] Windus et al.[6] and more recently Schwesinger and co-workers[7] predicted that **5a** would be more basic than **6a**, both of which would be more basic than their parent **7a**. The factors influencing the basicity of **6b** have also been recently analyzed.[7,8]

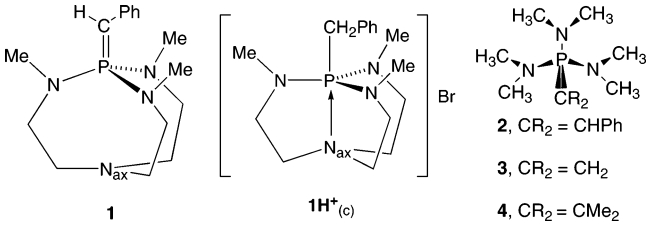

An interesting feature related to the strong basicity of phosphine **7** is the formation of a transannulated dative bond (from N_{ax} to phosphorus) as a result of protonation. In the case of **7** the protonation site is the phosphorus ($\mathbf{7H}^+_{(P)}$), while in the case of **5** and **6** this site is the CH_2 ($\mathbf{5H}^+_{(C)}$) and the phosphorus NH substituent ($\mathbf{6H}^+_{(N)}$), respectively. The formation of this transannular bond is thus expected to contribute to the predicted high basicity of **5**.[9]

No attempt has been made so far to quantitate this stabilization energy. The formation of the transannular bond is not only

[†] Budapest University of Technology and Economics.
[‡] Iowa State University.

(1) (a) Wang, Z.; Verkade, J. G. *Tetrahedron Lett.* **1998**, *39*, 9331−9334; (b) Wang, Z.; Zhang, G.; Guzei, I.; Verkade, J. G. *J. Org. Chem.* **2001**, *66*, 3521−3524.
(2) Goumri-Magnet, S.; Guettet, O.; Gornitzka, H.; Cazaux, J. B.; Bigg, D.; Palacios, F.; Bertrand, G. *J. Org. Chem.* **1999**, *64*, 3741−3744.
(3) Reynolds, K. A.; Dopico, P. G.; Brody, M. S.; Finn, M. G. *J. Org. Chem.* **1997**, *62*, 2564−2573.
(4) Mitzel, N. W.; Smart, B. A.; Dreihäupl, K.-H.; Rankin, D. W. H.; Schmidbaur, H. *J. Am. Chem. Soc.* **1996**, *118*, 12673−12682.
(5) $\mathbf{1H}^+_{(C)}$ is derived from **1** by protonation. **(C)** indicates that the protonation site is the carbon atom.
(6) Windus, T. L.; Schmidt, M. W.; Gordon, M. S. *J. Am. Chem. Soc.* **1994**, *116*, 11449−11455.
(7) Koppel, I. A.; Schwesinger, R.; Breuer, R.; Burk, P.; Herodes, K.; Koppel, I.; Leito, I.; Mishima, M. *J. Phys. Chem. A* **2001**, *105*, 9575−9586.
(8) Kovačević, B.; Barić, D.; Maksić, Z. B. *New. J. Chem.* **2004**, *28*, 284−288.

10.1021/ja0547533 CCC: $33.50

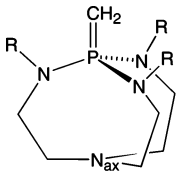

5a, R = H

5b, R = Me

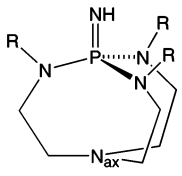

6a, R = H

6b, R = Me

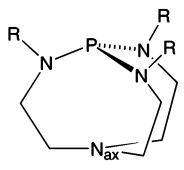

7a, R = H

7b, R = Me

7c, R = ^{i}Pr

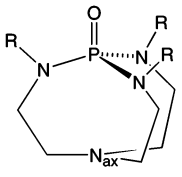

8a, R = H

8b, R = Me

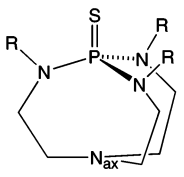

9a, R = H

9b, R = Me

associated with protonation. In the case of **7a** we found earlier that the corresponding radical cation has two bond stretch isomers (at the HF/6-31G* and MP2/6-31G* levels), the more stable one (by as much as 0.98 eV at MP2/6-31G*!) exhibiting a dative transannular bond.[10] Each of the two bond stretch isomers can be obtained by ionizing one of the two uppermost orbitals, which are the bonding and antibonding combinations of the P and the N_{ax} lone pairs. The "short-bond" cation is obtained from the antibonding combination by formally removing the electron from phosphorus, whereas the "long-bond" cation is obtained by formally removing the electron from the axial nitrogen. In some phosphatrane species (e.g., $\mathbf{6bH}^+_{(N)}$ and $\mathbf{8bH}^+_{(O)}$) two bond stretch isomers were also reported by others on the basis of HF/6-31G* calculations, although the energy difference between the two forms was small.[6]

Strong bases usually have a high-energy HOMO and thus a low ionization energy. This prompted us in our previous work[10] to investigate the photoelectron spectrum of **7b** and **7c**, which unlike **7a** are stable to isolation.[9a,b] The spectra were indeed characterized by a low first vertical ionization energy. It turned out, however, that due to the significantly reduced PN_{ax} distance of the radical cation (with respect to the neutral molecule), the calculated adiabatic ionization energy is even much lower (by ca. 1 eV below the vertical IE of **7a**), and could not be seen in the spectra as a result of the poor Franck−Condon factor.[10] Thus, these extremely low adiabatic ionization energies can be related to the formation of the transannular bond, which in turn can be related to the great basicity of these species. In a recent publication, Galasso confirmed our previous interpretation of the photoelectron spectra on the basis of OVGF calculations.[11] Very recently, it has been shown computationally that the lowest ionization energy of the closely related silatrane molecule

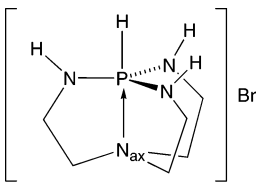

$\mathbf{7aH}^+_{(p)}$

depends strongly on the transannular SiN distance.[12] These ionization energy values were calculated by using the OVGF method on structures obtained by quantitized movement along the normal coordinate of the SiN vibration for the neutral silatrane. Optimization of the silatrane ionic states has not been performed.

Here we extend our photoelectron spectroscopic studies to the series **5**, **6**, **8**, and **9**. The photoelectron spectra of **8b** and **9b** were calculated by the OVGF method by Galasso.[11] Unfortunately, **5a** and **6a** would be very difficult to synthesize in view of the great proclivity of their precursor **7a** to polymerize.[9a,b] In this paper, we report the synthesis of **5b** and its characterization by NMR (^{1}H, ^{13}C, and ^{31}P) spectroscopy, and by X-ray crystallographic means. We also compare the relative basicity of **5b** and **7b**. Investigations of the structural and photoelectron spectroscopic properties of ylides **5b** and **6b**, together with those of the chalcogenides **8b** and **9b**, are reported herein in an effort to gain insight into the factors that determine the basicity of these systems. Quantum chemical calculations have also been carried out to interpret the photoelectron spectra of these compounds, and to gain a deeper understanding of the electronic as well as possible steric effects contributing to the basicity of the novel ylides **5b** and **6b**.

Results and Discussion

Synthesis of 5b. Initial attempts to deprotonate $\mathbf{5bH}^+_{(C)}$[13] with ^{t}BuOK in CH_3CN or with LDA in THF were not successful in allowing us to isolate **5b**. However, $\mathbf{5bH}^+_{(C)}$ upon treatment with five equivalents of sodium in liquid ammonia gave a residue, which upon extraction with pentane followed by crystallization from the same solvent, furnished **5b** as a colorless material in variable yield (11−40%). The low and variable yields are ascribed to incomplete conversions of $\mathbf{5bH}^+_{(C)}$ and/or hydrolysis of **5b** by adventitious water to which this compound is exceedingly sensitive. These synthetic difficulties are in accord with the predicted[6,7] great basicity of **5b**.

X-ray Structure Analysis of 5b. The molecular structure of **5b** (Figure 1) reveals the presence of a slightly distorted tetrahedral phosphorus center. While most of the structural parameters for the two different molecules observed [molecules 1 and 2] are close to each other (Table 1) the transannular PN_{ax} distances in the two molecules differ considerably (3.323 and 3.236 Å) even assuming an esd of 0.011 Å in each value, since the difference in distances is outside 3 × esd. The effect of the transannular PN_{ax} distance on the total energy of the proazaphosphatrane cages is rather small, as was shown by Windus et al.[6] Therefore, the subtle structural differences between molecules 1 and 2 of **5b** are not surprising and are very likely associated with crystal packing forces. Since these crystal forces are able to influence the PN transannular distance by nearly

(9) (a) Verkade, J. G. in, "$P(RNCH_2CH_2)_3N$: very strong nonionic bases useful in organic synthesis. New Aspects of Phosphorus Chemistry II" Majoral, J. P., Ed, *Top. Curr. Chem.* **2003**, *223*, 144. (b) Verkade, J. G.; Kisanga, P. *Tetrahedron* **2003**, *59*, 7819−7858. (c) Verkade, J. G.; Kisanga, P. "Recent Applications of Proazaphosphatranes in Organic Synthesis" *Aldrichimica Acta* **2004**, *37*, 3−14.
(10) Nyulászi, L.; Veszprémi, T.; D'Sa, B. A.; Verkade, J. G. *Inorg. Chem.* **1996**, *35*, 6102−6107.
(11) Galasso, V. *J. Phys. Chem.* A. **2004**, *108*, 4497−4504.
(12) Trofimov, A. B.; Zakrzewski, V. G.; Dolgounitcheva, O.; Ortiz, J. V.; Sidorkin, V. F.; Belogolova, E. F.; Belogolov, M.; Pestunovich, V. A. *J. Am. Chem. Soc.* **2005**, *127*, 986−995.
(13) Mohan, T.; Arumugam, S.; Wang, T.; Jacobson, R. A.; Verkade, J. G. *Heteroat. Chem.* **1996**, *7*, 455−460.

Table 1. Comparison of Salient Structural Features of **3**[a] and **5b**[b]

	3	**5b**	
parameters		molecule 1	molecule 2
distances, Å			
P−C	1.655(6)	1.6585(15)	1.6574(15)
$P-N_{eq}$[c]	1.666(4), 1.669(4)	1.6648(10), 1.6660(10)	1.6675(11), 1.6616(12)
	1.698(4)	1.6563(11)	1.6581(11)
$P-N_{ax}$[c]	-	3.323	3.236
angles, deg			
NPN	100.3(2), 99.0(2)	106.98(5), 106.51(5)	105.22(6), 104.96(5)
	114.7(2)	102.86(5)	107.99(6)
CPN	110.6(3), 109.4(3)	114.84(8), 114.95(8)	112.26(9), 111.05(8)
	122.4(4)	110.01(8)	115.61(7)
	120.4(4), 118.6(3)	122.84(8), 122.99(8)	123.46(9), 123.48(9)
PNC_{ring}[c]	122.4(4), 121.1(3)	123.41(8)	123.26(9)
	113.9(3), 114.3(3)		
PNC_{exo}[c]		120.31(9), 121.03(9)	119.8(9), 119.93(10)
		119.74(9)	120.43(10)
sum of NPN angles (deg)	314.0	316.4	317.3
sum of angles (deg)			
at N_{eq}[c]	355.6, 351.6, 337.3	359.8, 359.3, 358.7	359.4, 359.4, 359.8
at N_{ax}[c]		357.1	359.1

[a] Reference 4. [b] This work. [c] "Equatorial", "ring" and axial nitrogen notations do not apply to **3**.

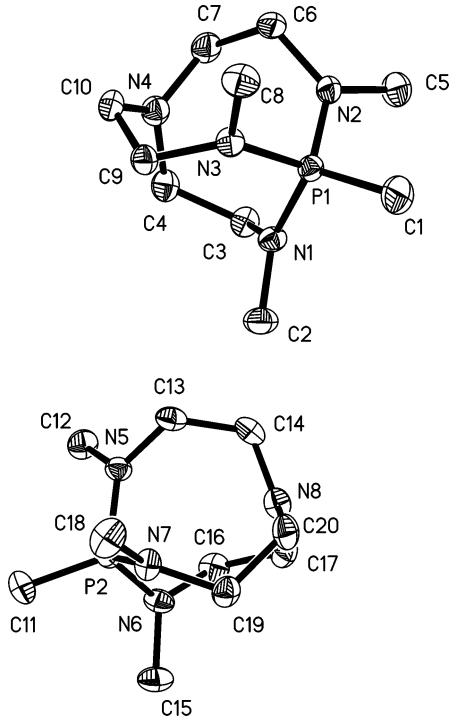

Figure 1. ORTEP diagram of **5b** was drawn at the 50% probability level. Hydrogen atoms were omitted for clarity.

0.1 Å (see Table 1), special care should be taken when comparing proazaphosphatrane transannular distances obtained from X-ray structures. Quantum chemical calculations, carried out at a uniform level of theory, are therefore very useful in predicting *relative* trends of transannular PN distances in related proazaphosphatrane cages. On the other hand the *absolute* values obtained from the calculatons are very sensitive to the level of theory applied as will be discussed below.

The P═C bond length in **5b** [1.659, 1.657 Å in molecules 1 and 2, respectively] is very close to that reported for **3** [1.655(6) Å].[4] Unlike **3**, wherein one of the nitrogens is non planar (angle sum around nitrogen = 337.3°), the geometry around the "equatorial" nitrogens in **5b** is virtually planar (sum of bond angles = 359.8, 359.3 and 358.7° in molecule 1; 359.4, 359.4, and 359.8° in molecule 2). Accordingly, the PN distances in **5b** (average 1.662 Å) are close to the analogous two PN distances in **3**, for which the nitrogens are planar (average 1.668 Å). The distance between the phosphorus and the non planar nitrogen of **3** is longer by 0.03 Å.

Structurally Imposed Bonding Considerations. The aforementioned structural characteristics indicate that the *lone pair of the non planar nitrogen* in **3** is less effective in back-bonding toward the antibonding $\sigma^*_{(PN)}$ MO-s than the other two nitrogens, resulting in an asymmetic structure. Woolins and coworkers have postulated that the planar amino group is "merely an electronegative atom bound to the phosphorus".[14] Mitzel et al.,[4] while noting that the "... precise origin (of the asymmetry) is still not clear..." stated that low symmetry (i.e., the non planarity of one of the nitrogens) is an inherent property of the $P(NR_2)_3$ skeleton in small molecules (R = Me).

The "inherent" low symmetry of the PN_3 units can be explained in the following way: The antibonding $\sigma^*_{(PN)}$ MO-s are good π acceptors and interact with the lone pair of the amino nitrogen.[15] The stabilization of this donor−acceptor interaction overcomes the planarization barrier of the amino nitrogen, resulting in planar nitrogens with shorter bond length. The phosphorus, however, becomes "saturated" by the back-donation of two nitrogens, and the stabilization achievable by the third back-donation is less than the planarization energy of the amino moiety. So the driving force for the non symmetrical arrangement is the inherent non planarity one of the amino groups. This description is supported by structural data for $[R-P(NMe_2)_3]^+$ species.[3] Such cations are symmetrical structures, because of the strong acceptor property of the cationic phosphorus which is then capable of accepting the donation of

(14) Clarke, M. L.; Holliday, G. L.; Slawin, A. M. Z.; Woollins, J. D. *J. Chem. Soc., Dalton Trans.* **2002**, 1093−1103.
(15) Murugavel, R.; Kumaravel, S. S.; Krishnamurthy, S. S.; Nethaji, M.; Chandrasekhar, J. *J. Chem. Soc., Dalton Trans.* **1994**, 847−852.

Table 2. Important Bond Lengths in Å and Bond Angle Sums (Σα) in Degrees of **5a**−**9a** at the HF/6-31+G* (normal font), B3LYP/6-31+G* (italics) and the MP2(full)/6-31+G* (bold) Levels of Theory

compound	P=E Å	P–N_{eq} Å	N_{eq}-C Å	C–C Å	C–N_{ax} Å	P–N_{ax} Å	Σα(N_{eq}) deg.	Σα(N_{ax}) deg.
		1.715	1.457	1.526	1.438	3.153	346.1	360.0
7a (E=lp)		*1.741*	*1.468*	*1.537*	*1.447*	*3.258*	*344.8*	*359.9*
		1.735	**1.466**	**1.522**	**1.442**	**3.011**	**343.6**	**357.5**
	1.471	1.677	1.454	1.525	1.444	2.823	347.4	355.8
8a (E=O)	*1.501*	*1.704*	*1.465*	*1.534*	*1.454*	*2.839*	*345.3*	*355.8*
	1.508	**1.699**	**1.461**	**1.520**	**1.454**	**2.657**	**343.5**	**349.5**
	1.971	1.678	1.457	1.525	1.443	2.867	348.2	356.8
9a (E=S)	*1.978*	*1.706*	*1.468*	*1.535*	*1.451*	*2.918*	*345.8*	*357.4*
	1.963	**1.700**	**1.464**	**1.520**	**1.452**	**2.713**	**344.0**	**351.0**
	1.555	1.694	1.459	1.525	1.441	2.913	348.2	357.6
6a (E=NH)	*1.574*	*1.705*	*1.465*	*1.539*	*1.448*	*3.064*	*348.0*	*359.6*
	1.579	**1.704**	**1.462**	**1.521**	**1.451**	**2.740**	**343.8**	**351.7**
	1.671	1.659	1.449	1.531	1.439	3.000	349.0	359.1
5a (E=CH_2)	*1.677*	*1.712*	*1.466*	*1.538*	*1.448*	*3.085*	*346.6*	*359.8*
	1.677	**1.705**	**1.462**	**1.524**	**1.447**	**2.831**	**345.8**	**354.4**

electron density from all three amino groups by overcoming their planarization energy. The gas-phase structure of O=$P(NMe_2)_3$ also has a C_s structure, although it has a 4.1 kcal/mol (MP2/6-31G*) preference for the C_3 structure.[16] This preference is smaller, however, than for **3**. Phosphorus in phosphonium cations as well as in phosphine oxides is a stronger electron acceptor than in **3** or in $P(NMe_2)_3$. It is worthy to note that the average P−N bond length in **5b** is somewhat shorter than that reported for **7c** [P−N = 1.703(1) Å].[17] This is also in accord with the above explanation; the phosphorus in **7c** being the weaker acceptor. It is also noteworthy that the difference in N-to-P back-donation between **5b** and **3** does not substantially affect the length of the ylidic P=C bond in these compounds (Table 1).

In contrast to the low symmetry in acyclic $E{=}P(N<)_3$ molecules, bicyclic proazaphosphatranes **7** = **E** have C_3 (**E**: lp, **O**, **S**) or quasi C_3 (**E: NH, CH_2**) symmetry. As a consequence of the symmetry imposed by the cage, each equatorial nitrogen lone pair participates rather equally in back-bonding toward phosphorus in the proazaphosphatranes. It is noteworthy that the three equatorial nitrogens are planar in all the X-ray structures reported for proazaphosphatranes, namely, **5b**, **7c**,[17] **8b**,[18] and **9b**.[19]

NMR Characterization of 5b. The constitution of **5b** was confirmed by HRMS and NMR (^{31}P, ^{1}H, and ^{13}C) spectroscopy as well as by X-ray crystallography, and its ^{1}H NMR spectrum is consistent with its structure. The ^{31}P NMR spectrum of **5b** revealed a peak at 65.0 ppm, somewhat upfield from that of **3** (δ_P 70 ppm).[3] The chemical shift for **5b** is 16.7 ppm downfield shift relative to that reported for $\mathbf{5bH^+_{(C)}}$ (δ_P 48.3 ppm).[13] The magnitude of this chemical shift difference is higher than that reported for **3** ($\Delta\delta_P$ 11.6 ppm) relative to $\mathbf{3H^+_{(C)}}$,[3,20] but lower than that reported for **1** relative to $\mathbf{1H^+_{(C)}}$ ($\Delta\delta_P$ 26.1 ppm).[1]

In contrast to the downfield δ_p value for **5b** relative to $\mathbf{5bH^+_{(C)}}$, an upfield shifted ^{31}P signal at 60.6 ppm was reported for **4** relative to that for $\mathbf{4H^+_{(C)}}$ (δ_P 65.0 ppm; $\Delta\delta_P$ −4.4 ppm).[2] A notable feature of the ^{13}C NMR spectrum of **5b** is a significantly higher $^{1}J_{PC}$ value of 366 Hz compared with those reported for **3** ($^{1}J_{PC}$ = 175 Hz) and **4** ($^{1}J_{PC}$ = 221 Hz).[1,3] The large difference in the $^{1}J_{PC}$ values of **3** and **5b** might be related to structural differences discussed above, although the origin of the coupling difference is presently obscure.

Table 3. Important Bond Lengths in Å and Bond Angle Sums (Σα) in Degrees of **5b**−**9b** at the HF/6-31+G* (normal font), B3LYP/6-31+G* (italics) and the MP2(full)/6-31+G* (bold) Levels of Theory

compound	P=E Å	P–N_{eq} Å	N_{eq}-C Å	C–C Å	C–N_{ax} Å	P–N_{ax} Å	Σα(N_{eq}) deg.	Σα(N_{ax}) deg.
		1.708	1.451	1.532	1.441	3.375[a]	359.9	357.9
7b (E=lp)		*1.733*	*1.458*	*1.544*	*1.457*	*3.439*[a]	*360.0*	*357.3*
		1.720	**1.452**	**1.531**	**1.444**	**3.412**	**360.0**	**357.6**
	1.468	1.664	1.453	1.532	1.440	3.194[b]	360.0	359.5
8b (E=O)	*1.497*	*1.687*	*1.461*	*1.544*	*1.449*	*3.275*[b]	*359.9*	*358.7*
	1.502	**1.676**	**1.454**	**1.531**	**1.441**	**3.161**[b]	**359.7**	**359.9**
	1.967	1.667	1.456	1.532	1.440	3.229[c]	360.0	359.1
9b (E=S)	*1.976*	*1.693*	*1.464*	*1.544*	*1.449*	*3.317*[c]	*360.0*	*358.2*
	1.953	**1.678**	**1.456**	**1.531**	**1.442**	**3.208**[c]	**360.0**	**359.6**
	1.551	1.672	1.454	1.533	1.441	3.249	359.9	359.0
6b (E=NH)	*1.573*	*1.697*	*1.462*	*1.544*	*1.450*	*3.334*	*359.9*	*358.0*
	1.573	**1.684**	**1.454**	**1.532**	**1.442**	**3.230**	**359.8**	**359.5**
	1.668	1.680	1.454	1.532	1.440	3.257[d]	359.3	358.9
5b (E=CH_2)	*1.676*	*1.710*	*1.464*	*1.544*	*1.449*	*3.297*[d]	*357.2*	*358.7*
	1.672	**1.696**	**1.459**	**1.531**	**1.440**	**3.144**[d]	**356.2**	**360.0**

[a] 3.293 Å in **7c** (X-ray, ref 16); 3.408 Å (MP2/6-31G*, ref 11). [b] 3.140 Å (X-ray, ref 17); 3.158 Å (MP2/6-31G*, ref 11). [c] 3.250 Å (X-ray, ref 18); 3.209 Å (MP2/6-31G*, ref 11). [d] 3.323 and 3.236 Å (X-ray, present work).

Structural and Bonding Features Obtained from ab Initio and Density Functional Calculations. In Tables 2 and 3, we summarize the important structural features obtained from ab initio calculations at different levels of sophistication for **5a**−**9a** and **5b**−**9b**, respectively. It was pointed out earlier[11,21] that the transannular distance in atranes depends strongly on the level of theory applied, and that large differences can occur between electron diffraction (gas phase) and X-ray (solid-state) structures. The present results for the **5a**−**9a** series clearly show that while the other bonding parameters exhibit only small changes, the transannular distance can vary by as much as 0.3 Å (see the MP2 and B3LYP results for **6a** in Table 2.), depending on the level of the theory used. The shortest P−N_{ax} distances are predicted at the MP2 level, whereas B3LYP provides the longest

(16) Mitzel, N. W.; Lustig, C. *J. Chem. Soc., Dalton* Trans. **1999**, 3177−3183.
(17) Wroblewski, A. E.; Pinkas, J.; Verkade, J. G. *Main Group Chem.* **1995**, *1*, 69−79.
(18) Tang, J.; Mohan, T.; Verkade, J. G. *J. Org. Chem.* **1994**, *59*, 4931−4938.
(19) Xi, S. K.; Schmidt, H.; Lensink, C.; Kim, S.; Wintergrass, D.; Daniels, L. M.; Jacobson, R. A. Verkade, J. G. *Inorg. Chem.* **1990**, *29*, 2214−2220.
(20) Schmidpeter, A.; Brecht, H. *Z. Naturforsch. B. Anorg. Chem. Org. Chem. Biochem. Biophys. Biol.* **1969**, *24*, 179−192.
(21) Kobayashi, J.; Goto, K.; Kawashima, T.; Schmidt, M. W.; Nagase, S. *J. Am. Chem. Soc.* **2002**, *124*, 3703−3712.

distances. The effect of the diffuse functions in the basis set used is less pronounced, resulting in a small but systematic shortening of the P−N_{ax} distance (the largest being the 0.036 Å shortening for **8a** with respect to Galasso's[11] MP2/6-31G* data). The equatorial nitrogens are pyramidal at all levels of the theory used, in agreement with the earlier HF[6] and MP2[11] results. Electronegative substituents at P clearly shorten the transannular distance at each level of theory, whereas the axial nitrogen remains nearly planar at the HF and B3LYP levels. However, at the MP2 level, the bond angle sums at the axial nitrogen in **5a**−**6a** and **8a**−**9a** are somewhat smaller than 360° (Table 2), in accordance with the shortened (by ca. 0.2−0.3 Å from the B3LYP and HF results) PN_{ax} distances. (The correlation between the PN_{ax} distance and the planarity at the axial nitrogen has been noted before.[11]) It seems that the interaction between phosphorus and the transannular nitrogen of the ring (which is in the axial position) is estimated to be stronger at the MP2 level than at HF or B3LYP.

For the systems with more bulky substituents, (**5b**−**9b**) the calculated structural data are collected in Table 3. The variation of the transannular bond lengths throughout the series is similar to that observed by Windus et al.[6] at the HF/6-31G* level of the theory. The equatorial nitrogens are planar at each level, in accordance with the available X-ray data for **5b**, **7c**,[17] **8b**,[18] and **9b**;[19] and with Galasso's MP2/6-31G* data for **7b**−**9b**.[11] The methyl-substituted cages **5b**−**9b** exhibit larger and more uniform transannular bond distances than the parent species **5a**−**9a**. This is in agreement with the earlier data obtained by Windus et al.,[6] and the MP2/6-31G* results of Galasso, in which the MP2/6-31G* P−N_{ax} distance in **8b** increased by nearly 0.5 Å from 2.693 Å in **8a**).[11] Also, the deviation between the present B3LYP/6-31+G* data and the MP2/6-31+G* results is much smaller than for the **7a**−**9a** series, the largest difference being 0.155 Å in the case of **5b**. Likewise for the **5a**−**9a** series, the MP2 transannular distance is consistently the shortest one. The calculated structural features are similar to those observed by X-ray crystallography for **5b**, **7c**,[17] **8b**,[18] and **9b**.[19] Particularly noteworthy is the agreement with the transannular PN_{ax} bond length, (which lies between 3.2 and 3.3 Å). While the present B3LYP/6-31+G* results predict longer transannular distances for **8b** and **9b** than their X-ray values by about 0.135 and 0.067 Å, respectively (see footnote in Table 3), and the agreement with the MP2/6-31+G* values is good, the B3LYP/6-31+G* result for **5b** lies between the experimental values for the two molecules in the solid-state structure of **5b** (see footnote in Table 3). The MP2/6-31+G* transannular distance for **5b** is shorter by 0.09 and 0.18 Å than those distances obtained from the solid-state structures of molecules 2 and 1 of **5b**, respectively. Noting the aforementioned sensitivity of the transannular distance to crystal packing forces, it is difficult to decide which calculated result is more reliable, and the previous (although cautious) preference for the MP2 calculations[11] should be considered with some reservation. If we consider that strong dipole−dipole interactions cause the solid phase structures to usually exhibit shorter distances between weakly bound atoms than in the gasous phase[22] (and this observation also holds for the SiN distance in silatranes[11,23]) then the B3LYP/6-31+G* level seems to provide even better results for the transannular bond than MP2, which predicts shorter distances than in the X-ray structure.

Table 4. Isodesmic Reaction Energies for Reactions **1a** and **1b** in Kcal/Mol at the HF/6-31+G* (normal font), B3LYP/6-31+G* (italics) and the MP2(full)/6-31+G* (bold) Levels of Theory

	reaction 1a for **7a**═**E**			reaction 1b for **7b**═**E**		
compound	HF	*B3LYP*	**MP2(full)**	HF	*B3LYP*	**MP2(full)**
7a−**b** (E═lp)	−1.7	*4.2*	**11.8**	−5.9	*−1.7*	**16.8**
8a−**b** (E═O)	1.9	*4.1*	**15.8**	−0.6	*2.6*	**22.1**
9a−**b** (E═S)	2.6	*4.5*	**20.2**	−2.5	*0.6*	**22.9**
6a−**b** (E═NH)	−0.2	*1.5*	**14.1**	−5.0	*−1.4*	**18.2**
5a−**b** (E═CH_2)	−0.8	*1.0*	**13.9**	−6.1	*−2.0*	**18.4**

The longer transannular distance in methylated **5b**−**9b** has a corresponding structural effect on the planar equatorial nitrogens. Together with the greater planarity of the equatorial nitrogens, the P−N_{eq} distances are consequently somewhat shorter in the **6b**−**9b** than in the **6a**−**9a** series (cf. the B3LYP/6-31+G* results in Tables 2 and 3). Because of the increased planarity (owing to methyl substitution), the lone pairs of the equatorial nitrogens in **6b**−**9b** ought to function as better electron donors toward phosphorus than when these nitrogens are non planar. It can be assumed that the inductive effect of the methyl substituents at N_{eq} also increases the donor ability. The P−N_{eq} distances in **5b** have the smallest shortening with respect to **5a** in the presently investigated series. Apparently, the CH_2 group at phosphorus is the best electron donor among the E substituents investigated, and the back-donation of the nitrogens is less effective in this case. It seems that there is an inverse correlation between the electron donation from the equatorial nitrogens and the donation from the axial nitrogen. The P−N_{ax} distance is the parameter that is the most sensitive to the level of theory applied; a result that is consistent with the flexibility of the ring.

To assess the energetic effect of the closure of the atrane cage, the isodesmic reaction 1 was employed.[24] Stabilization in reaction 1 can be taken as an indicator of the formation

7a═E + 3 NH_3 + 3 CH_4 → Et_3N + 3 $MeNH_2$ + E═$P(NH_2)_3$ (1a)

7b═E + 3 NH_3 + 3 CH_4 → Et_3N + 3 $MeNH_2$ + E═$P(NHMe)_3$ (1b)

of a new bond in the cage, which is not present in the fragments. Destabilization would be an indicator of ring strain. For **5a**−**9a**, the energy of the isodesmic reaction (Table 4) is near zero at the HF/6-31+G* and at the B3LYP/6-31+G* levels of the theory. At the MP2/6-31+G* level, however, some stabilization (10−20 kcal/mol, Table 4) is obtained, a result that can be attributed to the formation of a transannular bond. This surmise is reinforced by the fact that the shortest P−N_{ax} bonds are exhibited for the **5a**−**9a** series at the MP2 level. Thus, we carried out CCSD/cc-PVDZ//B3LYP/6-31+G* calculations on isodesmic reaction 1a in the case of **7a**. The 7.6 kcal/mol stabilization (which is between that of the B3LYP and the MP2

(22) Jiao, H.; Schleyer, P. v. R. *J. Am. Chem. Soc.* **1994**, *116*, 7429−7430; Leopold, K. R.; Canagaratina, M.; Phillips, J. A. *Acc. Chem. Res.* **1997**, *30*, 57−64; Mitzel, N. W.; Losehand, U.; Wu, A.; Cremer, D.; Rankin D. W. H. *J. Am. Chem. Soc.* **2000**, *122*, 4471−4482.

(23) Greenberg, A.; Wu, G. *Struct. Chem.* **1990**, *1*, 79−85.

(24) Galasso (ref 11) has used a somewhat different isodesmic reaction scheme for **7a** and $\mathbf{7aH^+_{(P)}}$, and concluded that there is no difference between the strain of the neutral and the protonated systems.

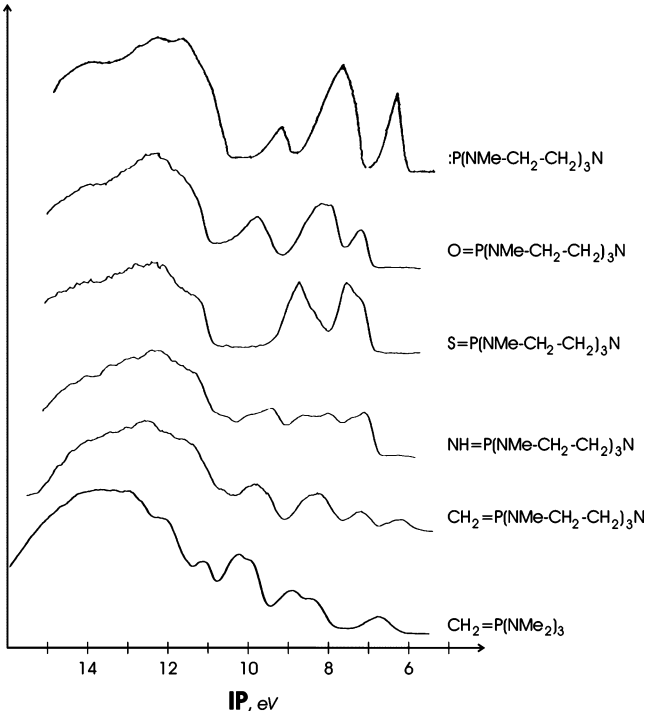

Figure 2. He I Photoelectron spectra of the investigated compounds.

result) indicated that there is a small amount of stabilization of the cage. This finding is in agreement with the known flexibility of the cage.[6] It is worth noting here that the minimum-energy structure of triethlyamine (and also of triethanolamine) has C_3 symmetry, and that the nitrogen lone pair is in the endo position,[25] as is also the case in the cage compounds with the transannulated bonds.[26] Moreover, no transannular bond has been reported for the neutral systems **5b**−**9b**.[27]

Photoelectron Spectroscopic Results. The He−I photoelectron spectra of the **5b**−**9b** series and **3** are shown in Figure 2. Ylide **5b**, as expected, has the lowest first ionization energy (6.30 eV) among the compounds investigated. This value is somewhat lower than the vertical ionization energy of **7b** (6.61 eV). Phosphorus ylides are known to have low ionization energies[28] corresponding to the removal of the electron from their π-type orbital localized to a large extent at the carbon, providing the ylidic character of the system.[29] The first ionization energy of **5b** is even lower than the value reported for $Me_3P{=}CH_2$ (6.82 eV)[28] or the ionization energy of $(Me_2N)_3P{=}CH_2$ (**3**, 6.7 eV, see below). The first vertical ionization energies of **6b**, **8b**, and **9b** are higher than that of **7b**.

To support the assignment of the spectra, HF/6-31+G*// B3LYP/6-31+G* calculations were carried out. The lowest lying Koopmans ionization energies, together with the measured values, and the orbitals of **8a** (as representative for the whole series of compounds plotted by the MOLDEN program)[30] are shown in Table 5. In the case of **7b**, the HOMO and the NHOMO were assigned to the combination of the phosphorus lone pair and the lone pair at the axial nitrogen.[10] This assignment was later confirmed by the OVGF calculations of Galasso.[11]

Table 5. HF/6-31+G*// B3LYP/6-31+G* Koopmans Ionization Energies and Measured Vertical Ionization Energies (in bold), the First Ionization Energies are Given in Italics

Compound	$\pi_{P=E}$ [a]	$n_{N_{ax}}$ (+n_N) [a]	n_N (+ $n_{N_{ax}}$) [a]	n_N [a]
7b (E= lp)	7.64 ***6.61*** [b]	9.18 **8.0** [c,b]	10.85 **9.5** [b]	9.55 [d] **8.0** [c]
8b (E= O)	11.64 [d]	8.83	10.32	9.90 [d]
9b (E= S)	**10.03** 8.55 [d]	***7.52*** 8.85	**8.5** [c] 10.31	**8.5** [c] 10.42 [d]
6b (E= NH)	**7.84** 8.92	***7.4 sh*** 8.67	**8.5** *sh* 10.17	**8.97** 10.24, 10.90
5b (E= CH_2)	**7.7** *sh* 7.09 ***6.30***	***7.32*** 8.62 **7.26**	**8.23** 10.01 **8.3** [c]	**8.95, 9.67** 9.75, 10.26 **8.3** [c]

[a] The orbitals shown are those of **8a**, for illustrative purposes. [b] The first two ionizations of **7b** were assigned[10] to the combinations of the lone pairs of phosphorus and the axial nitrogen, with some contribution from the equatorial nitrogen lone pairs, as shown on the third orbital. [c] denotes broad and intense band, indicating more than one ionization. *sh* denotes a shoulder [d] denotes a degenerate orbital.

The two uppermost orbitals of **5**, **6**, **8**, and **9** are the N_{ax} lone pair,[31] and the "ylidic" orbital localized at the exocyclic E substituent of phosphorus. (See the first two columns in Table 5). For **8a** and **8b**, the doubly degenerate ylidic orbital is strongly mixed with the $P{-}N_{eq}$ orbitals having the proper symmetry, and in the case of **8b**, the ylidic pair of orbitals can preferably be assigned to the more stable bonding combination. The HF/6-31+G*//B3LYP/6-31+G* energy of the "ylidic" orbital in the case of **5b** is −7.09 eV. The increasing electronegativity of the phosphorus E substituent is stabilizing (down to −11.64 eV in the case of **8b**).

The HOMO is separated by more than 1 eV from the other orbitals in **5b** and **8b**, allowing rather firm assignments of these MOs. For **6b** and **9b**, however, this energy separation is small, rendering the Koopmans theorem-based assignment dubious. The calculated Koopmans N_{ax} lone pair ionization energy is nearly constant for compounds **5b**, **6b**, **8b**, and **9b**. This finding is in agreement with the observation that for **5b** and **6b** as well as for **8b** and **9b,** the $P{-}N_{ax}$ distance is between 3.2 and 3.3 Å, and one can expect that the N_{ax} lone pair remains relatively unperturbed by the corresponding changes in the phosphorus substituent. Indeed, the first IE of **8b** and the second IE of **5b** (both assignable to the N_{ax} orbital on the basis of the calculations − see above) are at similar ionization energies (7.52, 7.4, 7.32, and 7.26 eV, for **8b**, **6b**, **9b**, and **5b,** respectively). Since the

(25) Párkányi, L.; Hencsei, P.; Nyulászi, L. *J. Mol. Struct.* **1996**, *377*, 27−33.
(26) In the neutral proazaphosphatranes the axial nitrogen is virtually planar, in contrast with the triethylamine structure. This planarity might be attributed to the constrained structure of the cage. This planarity has also been attributed to van der Waals interactions among the hydrogens on the methylene carbons adjacent to N_{ax}. (See Clardy, J. C.; Milbrath, D. S.; Verkade, J. G. *J. Am. Chem. Soc.* **1977**, *99*, 631−633, and references therein.) This explanation, however, does not account for the concave topology of triethylamine and triethanolamine.
(27) In refs 6 and 11, the electron density was investigated using the method developed by Bader. For most of the neutral systems, bond critical points were obtained between P and N_{ax}. The electron densities at these critical points were very small, indicating a weak covalent interaction.
(28) Ostoja Starzewski, K. A.; Bock, H. *J. Am. Chem. Soc.* **1976**, *98*, 8486−8494.
(29) Nyulászi, L.; Veszprémi, T.; Réffy, J. *J. Phys. Chem.* **1995**, *99*, 10142−10146.
(30) Schaftenaar, G.; Noordik, J. H. "Molden: a pre- and post-processing program for molecular and electronic structures", *J. Comput.-Aided Mol. Design* **2000**, *14*, 123−134.
(31) Note that the three equatorial nitrogen lone pairs (in C_3 local symmetry) form an a_1 and an e combination. The a_1 combination is of proper symmetry to interact with the N_{ax} lone pair. (See the orbitals in Table 5).

N_{ax} ionization energy is thus in the 7.3−7.5 eV region, we assign the 7.32 eV and 7.4(sh) features of **7b** and **9b**, respectively, to this orbital, interchanging the calculated (Koopmans) ordering of the first two closely lying ionizations of these compounds. Further support is given to this assignment by the relative intensities of the spectrum of **9b**, since the 7.4 eV shoulder is clearly a single ionization while the 7.84 eV maximum originates from a doubly degenerate orbital of sulfur. The OVGF calculations of Galasso[11] also predict the first ionization of **9b** (7.40 eV) as originating from the axial nitrogen lone pair, in excellent numerical agreement with experiment. To provide further support to this assignment, we compared the spectrum of **5b** to that of **3** (see Figure 2). The two spectra are quite similar, with the exception of the extra band at 7.26 eV in the spectrum of **5b** (supporting its assignment to the lone pair of the axial nitrogen) which, as expected, ought to be absent from the spectrum of **3**. The similar position of the bands (with the apparent exception of the N_{ax} lone pair, and the small lowering of the first ionization energy) provides further evidence that in the case of **5b** there is no sizable interaction between the phosphorus and the axial nitrogen lone pair (see above). Such an interaction should have resulted in splitting of the energy levels.

Considering the aforementioned small variation of the N_{ax} lone pair energy throughout the investigated series of molecules **5b**, **6b**, **8b**, and **9b** (IE: 7.3−7.5 eV, see above), it becomes apparent that phosphorus is not interacting appreciably in any of the proazaphosphatrane ylides (**5b**, **6b**, **8b**, and **9b**) with the axial nitrogen lone pair. Also, the shape of this orbital (see Table 4) indicates that it is localized at N_{ax} (with small contributions from the CC bonds but not from phosphorus). Thus, the corresponding ionization energies (7.3−7.5 eV) should be similar in value to that in a planar trialkylamine. (Recall the virtually planar carbon arrangement about the axial nitrogen in all the prozazphosphatrane compounds we studied.) Nitrogen is pyramidal in most amines and thus the lone pair has some "s" character. The pure "p" orbital of a planar amine is less bound than in a corresponding sp^3 hybrid, and thus the corresponding ionization energy should be lower than for compounds with a pyramidal nitrogen. Although the Et_3N lone pair has an ionization energy of 8.08 eV,[32] for manxine [$N(CH_2CH_2CH_2)_3CH$], a cage compound with a planar nitrogen, an ionization energy of 7.05 eV has been reported.[33] This value is somewhat lower than the 7.3−7.5 eV values for the N_{ax} lone pair in the substituted proazaphosphatranes and the difference can be at least partially explained by considering the electron withdrawing effect of the equatorial nitrogens in the ring.

The first two ionizations of **7b** were assigned to the bonding and antibonding combinations of the P and the N_{ax} lone pairs, respectively,[10,11] although there is also some interaction with one orbital formed from the equatorial nitrogen lone pairs of proper symmetry. The corresponding two ionization energies of **7b**, as is usual for orbital combinations, are at higher (8.0 eV) and lower (6.61 eV) ionization energies, for the bonding and antibonding MOs, respectively, than the unperturbed N_{ax} lone pair ionization energy. (This can be estimated to be about 7.3 eV on the basis of the photoelectron spectra of the substituted proazaphosphatranes **5b**, **6b**, **8b**, and **9b**, where virtually no interaction with a phosphorus lone pair is possible − see above.) The rather low first vertical ionization energy value of **7b** (6.61 eV) is thus a consequence of this orbital interaction. The assignments of the remaining low-lying bands of **5b**, **6b**, **8b**, and **9b** are based on the calculated Koopmans values, and the relative intensities (for **8b** and **9b**, where degenerate energy levels are present) are given in Table 5. Further support for the assignment of the remaining low lying bands is provided by the near constant value of the combination of the N_{eq} lone pairs.

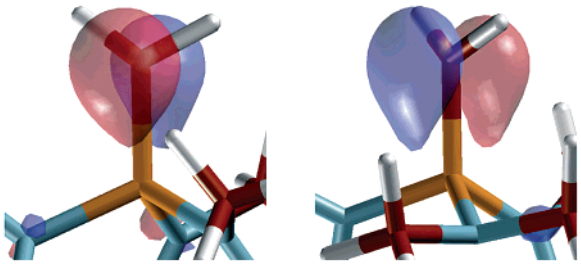

5b **3**

Figure 3. Kohn−Sham HOMO of **5b** and **3**.

Removal of the electron from the orbital at the phosphorus substituent results in a cationic ground state for **5b** only. This ionization energy is even lower (6.30 eV) than that of **3**, which itself has a rather low ionization energy value (6.70 eV), in agreement with the high predicted basicity of **5b**.[7] In the case of **7b**, the lowering of the phosphorus lone pair ionization energy (with respect to that of $P(NMe_2)_3$) was attributed to an interaction with the N_{ax} lone pair.[10] The explanation of the lowering of the ylidic ionization energy for **5b** (with respect to that of **3**) is much less straightforward, since the N_{ax} orbital points toward the PC σ bond, whereas the ylidic type orbital is perpendicular to this bond (according to the orbital plots in Table 5) and the interaction between them is negligible on symmetry grounds. Recalling the structural difference between **5b** and **3**, the destabilization of the ylidic orbital in **5b** is understandable. The three planar equatorial nitrogens in **5b** "saturate" the electron demand of phosphorus, thus the stabilizing π-type back-bonding from the CH_2 group is less effective in this compound than in **3**, where one of the substituting nitrogens is non planar (see above) leaving the possibility for a stronger back-donation from the ylidic carbon. The plots of the HOMO-s of **5b** and **3** shown in Figure 3 support this conclusion. It should be noted, however, that the P═C bond lengths in **5b** and **3** are close to each other (Table 1.). Apparently, this parameter is less sensitive to the changes in the ylidic bonding.

Ylide **5a** has the highest predicted basicity[6,7] among **5a**−**9a**, in agreement with the fact that **5b** has the lowest ionization energy among **5b**−**9b**. However, **6a**, has been predicted to have a gas-phase basicity that is higher than that of **7a**,[6,7] although the first IE value of **7b** is significantly lower (by 0.7 eV) than that of **6b**. From a recent investigation[34] it turned out that the basicity of **6b** is smaller than that of **7b** in acetonitrile solution. To understand this seeming contradiction, we should consider that basicity corresponds to the energy difference of the base and its protonated form, each in their *equilibrium* geometry.

(32) Takahashi, M.; Watanabe, I.; Ikeda, S. *J. El. Spectrosc. Relat. Phenom.* **1985**, *37*, 275−290.
(33) Aue, D. H.; Web, H. M.; Bowers, M. T. *J. Am. Chem. Soc.* **1975**, *97*, 4136−4137.
(34) Liu, X.; Thirupathi, N.; Guzei, I. A.; Verkade, J. G. *Inorg. Chem.* **2004**, *43*, 7431−7440.

Table 6. Important Bond Lengths and Bond Angle Sums (Σα) at the Equatorial Nitrogens of Short Bond Radical Cations **5a**$^{*+}$−**9a**$^{*+}$ and **5b**$^{*+}$−**9b**$^{*+}$ at the HF/6-31+G* (normal font), B3LYP/6-31+G* (italics), and the MP2(full)/6-31+G* (bold) Levels of Theory[a]

compounds	**5a**$^{*+}$−**9a**$^{*+}$					**5b**$^{*+}$−**9b**$^{*+}$				
	P=E Å	P–N_{eq} Å	P–N_{ax} Å	Σα(N_{eq}) deg.	$\Delta E_{S/L}$ kcal/mol	P=E Å	P–N_{eq} Å	P–N_{ax} Å	Σα(N_{eq}) deg.	$\Delta E_{S/L}$ kcal/mol
		1.660	2.095	354.1	7.2		1.672	2.036	354.9	14.7
7^{*+} (E=lp)		*1.690*	*2.199*	*352.0*	*−1.7*		*1.706*	*2.109*	*352.7*	*−1.6*
		1.686	**2.062**	**350.7**	**21.6**		**1.698**	**2.025**	**349.7**	**27.0**
	1.454	1.703	2.687	357.4	−14.1	1.455	1.638	2.906	359.0	−5.6
8^{*+} (E=O)						*1.496*	*1.727*	*2.449*	*359.7*	*−6.4*
	1.498	**1.722**	**2.372**	**358.9**	**−11.5**	**1.506**	**1.753**	**2.215**	**359.3**	**−5.6**
	2.144	1.652	2.124	356.3	7.5	2.101	1.635	2.742	358.8	4.7
9^{*+} (E=S)	*2.143*	*1.682*	*2.169*	*356.9*	*3.4*	*2.165*	*1.708*	*2.116*	*357.9*	*−9.9*
	2.148	**1.677**	**2.058**	**354.3**	**18.2**	**2.110**	**1.660**	**2.488**	**356.1**	**9.3**
	1.726	1.654	2.113	356.1	21.8	1.700	1.636	2.675	358.5	18.0
6^{*+} (E=NH)	*1.744*	*1.683*	*2.135*	*354.1*	*9.1*	*1.691*	*1.667*	*2.680*	*358.3*	*1.7*
	1.746	**1.677**	**2.052**	**353.4**	**21.5**	**1.726**	**1.666**	**2.385**	**355.1**	**13.0**
	1.802	1.655	2.263	354.4	45.8	1.785	1.642	2.794	358.7	45.4
5^{*+} (E=CH_2)	*1.813*	*1.688*	*2.220*	*353.4*		*1.788*	*1.669*	*2.773*	*358.0*	
	1.808	**1.682**	**2.119**	**352.7**	**50.6**	**1.788**	**1.664**	**2.571**	**358.0**	**43.5**

[a] ΔE is the energy difference between the short and long bond structures.

Vertical ionization energies, however, correspond to energy differences between the neutral species and their corresponding radical cations *without any geometry relaxation*. We have already noted that the vertical and the adiabatic ionization energies are considerably different for **7b**.[10] This difference was attributed to the stabilization of the radical cation by the formation of a strong transannular bond not present in **7b**, which also leads to huge geometry changes involving shortening of the P−N_{ax} distance by as much as 1 Å. Since protonation is also known to result in large changes in the P−N_{ax} distance,[5,9] we investigated the minimum energy structure of the radical cations of **5**−**9** to understand the unexpected difference between the basicity and the ionization energy trends within the series of compounds studied herein.

Structures of the Radical Cations. In contrast to neutral **5a,b**, **6a,b**, **8a,b**, and **9a,b**, where only a single minimum was obtained, two radical cation structures were found at the HF/6-31+G* and at the MP2/6-31+G* levels of the theory for each of the aforementioned series of compounds, as was the case in our earlier findings for **7a**.[10] The most striking difference between the structures of the two bond stretch isomers **5a**$^{+\bullet}$−**9a**$^{+\bullet}$ is in their transannular P−N_{ax} distance. The isomer with a short (2.1−2.8 Å) P−N_{ax} possesses a pyramidalized axial nitrogen. Moreover, the P=E bond elongates by 0.13−0.2 Å and the P−N_{eq} bond shows a slight shortening with respect to the neutral state of these structures. These geometrical features resemble the protonated forms of the proazaphosphatrane bases.[6,11] The most pertinent structural data for the short bond **5a**$^{+\bullet}$−**9a**$^{+\bullet}$ and **5b**$^{+\bullet}$−**9b**$^{+\bullet}$ radical cationic series are collected in Table 6. The other bond stretch isomers with the long transannular bond have structural characteristics similar to those of the corresponding neutral base (see structural data tabulated in the Supporting Information in Table S1). At the B3LYP/6-31+G* level, **8a**$^{+\bullet}$ and **8b**$^{+\bullet}$ have only a long-bond, while **5a**$^{+\bullet}$ and **5b**$^{+\bullet}$ have only a short-bond cation structure. Attempts to locate their isomeric counterparts were unsuccessful.

To our great surprise, the most stable B3LYP/6-31+G* structure for **7a**$^{+\bullet}$ (by 1.7 kcal/mol) has a long P−N_{ax} distance, while no such minimum could be located earlier at the BLYP/6-31G* level.[10] On the contrary, at the MP2/6-31G* level the structure with the short bond was more stable by as much as 21.7 kcal/mol![10] A characteristic feature of the B3LYP/6-31+G* structure with the long transannular bond is that the P−N_{eq} distances are shorter than in the MP2 and HF structures, and the equatorial nitrogens are flattened (Table 6). This indicates that removal of the electron occurred from the phosphorus lone pair, and the resulting radical cation was stabilized by electron donation from the three equatorial nitrogens, instead of from the axial one. The plot of the Kohn−Sham SOMO indeed reveals that this is the case. Re-optimization of the B3LYP/6-31+G* structure with the long transannular distance at the MP2/6-31+G* level resulted in the previously obtained long transannular bond radical cation. To the contrary, reoptimization at the HF/6-31+G* level resulted in the more stable radical cation with the short transannular bond. This shows that the description of the stabilizing interaction between the phosphorus radical cation and the axial nitrogen is less pronounced at the B3LYP than at the HF and MP2 levels for **7a**$^{\bullet+}$. We should recall here that in the **5a**−**9a** series, the transannular distances were always the longest at the B3LYP level (Table 2). CCSD(T)/cc-PVDZ//B3LYP/6-31+G* calculations on **5a**$^{+\bullet}$ showed that the structure stabilized by the equatorial nitrogens is 8.9 kcal/mol higher in energy than the radical cation with the short axial bond. Taking the coupled cluster calculations as a benchmark, we can conclude that at the density functional level used here, the interaction of phosphorus with the equatorial nitrogens is overestimated, while at the MP2 level it is underestimated.

The short-bond radical cation is thus more stable then its long-bond counterpart in the series studied, with the exception of **8a**$^{+\bullet}$. This stabilization energy difference is the largest for **5a**$^{+\bullet}$ (50 kcal/mol at the MP2/6-31+G* level). For **6a**$^{+\bullet}$ and **9a**$^{+\bullet}$ the preference of the short-bond cation is reduced to about 20 kcal/mol, while for **8a**$^{+\bullet}$, the long-bond cation is the more stable one (by 1.8 kcal/mol at the MP2/6-31+G*, Table 6). The structures which could not be optimized at the B3LYP/6-31+G* level (i.e., long-bond **8a**$^{+\bullet}$ and short bond **5a**$^{+\bullet}$) were always the least stable at the MP2/6-31+G* level.

Inspection of the NBO partial charges (see Table S2 Supporting Information) reveals that for the short-bond cation, the charge changes mainly at the axial substituent of the phosphorus upon ionization, while for the long-bond cations the largest

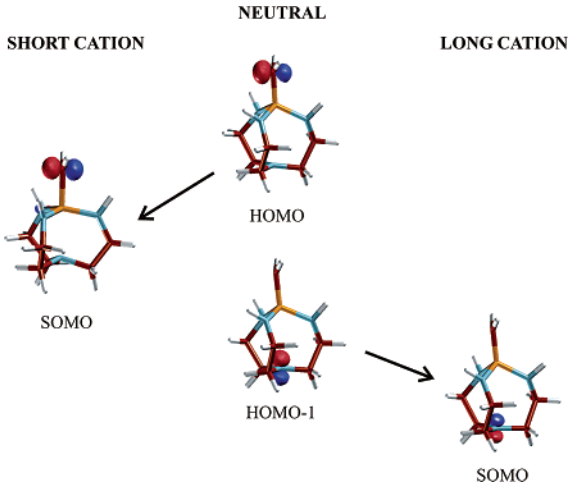

Figure 4. Highest occupied orbitals of the short-bonded and long-bonded radical cations of **7**═**E** type molecules as derived from the HOMO and HOMO-1 orbitals of the parent **7**═**E**.

increase of the charge is at the axial nitrogen. Accordingly, the SOMO of the long-bond radical cation is the axial nitrogen lone pair, whereas for the short-bond radical cation the electron was removed from the phosphorus substituent. The SOMO-s of the short- and the long-bond cations of $\mathbf{5a}^{+\bullet}$ are shown together with the two uppermost MO-s of **5a** in Figure 4. From an inspection of the shape of the MO-s, it is apparent that the orbital at the axial nitrogen is hardly influenced by electron removal. The ylidic MO, localized mainly at the substituent of the phosphorus, however, changes substantially upon ionization. The SOMO of the short-bond radical cation is clearly localized at the phosphorus substituent (i.e., the carbon in Figure 4), whereas in the case of the parent neutral, the corresponding orbital is much more polarized toward the phosphorus, in agreement with the π-back-bonding concept generally used to describe the bonding in the phosphorus ylides.[35] This π-back-bonding is less effective with increasing electronegativity of the axial substituent atoms of the phosphorus ylides. In a phosphine oxide (e.g., **8a**), even the orbital of the neutral is localized mainly at the oxygen atom (see the shape of that orbital as represented in Table 5). The ellipticity of the PX bond calculated by Bader's method[36] decreases from 0.44 and 0.19 (in **5a** and **6a**, respectively) to 0.05 and 0.01 in the corresponding short-bonded radical cation as an indication of diminished π back-bonding. As a consequence, the P═E distance in the short-bond radical cations elongates considerably with respect to the neutral (Tables 3, 4, and 6) as mentioned above.

The positive partial charge of the phosphorus in the short-bond cation differs only slightly from that in the neutral. Apparently, the electron density lost by the diminished π back-donation is compensated. In the case of the radical cations, this occurs mainly by the formation of the transannular bond in which electrons are donated from the lone pair of the axial nitrogen. It is worthy to note that the increased back-donation from the equatorial nitrogens is an alternative possibility, as is indicated by the stability of the B3LYP/6-31+G* structure of $\mathbf{7a}^{+\bullet}$ that possesses a long transannular bond (see above).

For the methylated series $\mathbf{5b}^{+\bullet}$–$\mathbf{9b}^{+\bullet}$ the stabilization by the equatorial nitrogens is even more pronounced. Both HF and

(35) Bestmann, H. J.; Kos, A. J.; Witzgall, K.; Schleyer, P. v. R. *Chem. Ber.* **1986**, *119*, 1331–1349.
(36) Bader, R. W. F. *Acc. Chem. Res.* **1985**, *18*, 9–15.

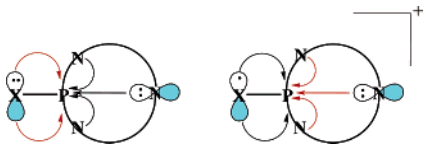

Figure 5. Schematic representation of the effects compensating for the electron deficit at phosphorus upon ionization at E.

B3LYP data from Table 6 clearly show that the transannular distance in $\mathbf{5b}^{+\bullet}$, $\mathbf{6b}^{+\bullet}$, and $\mathbf{9b}^{+\bullet}$ is longer by about 0.5 Å than in $\mathbf{5a}^{+\bullet}$, $\mathbf{6a}^{+\bullet}$, and $\mathbf{9a}^{+\bullet}$, respectively, and the equatorial nitrogens are flattened by the methyl substitution. Nevertheless, this transannular distance is still shorter by about 0.5 Å than in the neutral molecules (**5b**–**9b**, see Table 3 and Table 6). Since the same behavior can be seen at all levels used, it is unlikely to be attributed to a computational artifact. The effect of methylation is much less pronounced in the long bond cations. Other examples of this type of interaction will be discussed below for the case of cations obtained by protonation. The "mechanism" to saturate the electron demand of phosphorus possessing a partial positive charge is shown in Figure 5.

Since the short-bond and the long-bond cations formed by **5**–**9** are created by ionizing the ylidic and the axial nitrogen lone pair MO-s their relative stabilities should be related to the difference between the ionization energies of the ylidic and the nitrogen axial lone pair orbitals. For $\mathbf{8b}^{+\bullet}$ the short-bond and the long-bond cations have nearly identical energies (Table 6, MP2/6-31+G*), while the ionization energy of the ylidic orbital (combined with the N_{eq} MO-s of proper symmetry) is larger by 1 eV than the ionization of the axial nitrogen (see above). Thus, one might surmise that the stabilization energy in the short-bond radical cation of $\mathbf{8b}^{+\bullet}$ is about 1 eV (23 kcal/mol). Assuming similar stabilization for each short-bond cation, the long bond cation of $\mathbf{5b}^{+\bullet}$ should be less stable than its short-bond counterpart by $2 \times 23 = 46$ kcal/mol, since the ionization energy of the ylidic orbital in **5b** is about 1 eV (23 kcal/mol) lower than that of the axial lone pair ionization (see Table 5). The two ionization energies are close to each other in **6b** and **9b**, the ionization of the axial nitrogen lone pair being favored by about 0.4 eV (10 kcal/mol). Using the same considerations employed for **5b** the short-bond cation in each of these molecules should be more stable than the long-bonded one by about 13 kcal/mol. The calculated relative energies in Table 6 are in reasonable agreement with the values obtained from the aforementioned assumptions.

The stabilization of the short-bond radical cations (which is related to the formation of the transannular bond) can also be estimated using isodesmic reaction energies. In agreement with the short transannular bond, the stabilization of the short bond cations is substantial according to the isodesmic reaction 2. The isodesmic reaction energies for reactions 2a and 2b (i.e., for the short bond cations) are presented in Table 7, while for the long bond cations (reactions 3a and 3b) the data are collected in Table 8. The energies of reaction 3 for the long bond cations in Table 8 are smaller than the energies of reaction 2. Likewise for the neutral systems, some stabilization is obtained at the MP2 level of the theory. Subtracting the energies of reactions 3 and 1, we obtain a homodesmotic reaction. This reaction compensates for ring strain, and its energy is close to zero at each level of the theory. The energies of reaction 2b are smaller than the energies of reaction 2a, in agreement with the longer

Table 7. Isodesmic Reaction Energies for Reactions **2a** and **2b** in kcal/mol at the HF/6-31+G* (normal font), B3LYP/6-31+G* (italics), and the MP2(full)/6-31+G* (bold) Levels of Theory

	reaction 2a for **7a**=**E**$^{+\bullet}$			reaction 2b for **7b**=**E**$^{+\bullet}$		
compound	HF	*B3LYP*	**MP2(full)**	HF	*B3LYP*	**MP2(full)**
7a−**b** (E=lp)	24.2	*23.3*	**42.4**	18.3	*16.8*	**44.6**
8a−**b** (E=O)	30.1	-	**44.8**	17.5	*20.0*	**38.7**
9a−**b** (E=S)	22.2	*24.7*	**44.6**	9.6	*5.7*	**38.1**
6a−**b** (E=NH)	20.9	*23.8*	**41.4**	10.5	*12.7*	**37.9**
5a−**b** (E=CH_2)	15.8	*19.3*	**36.4**	8.4	*11.6*	**35.1**

Table 8. Isodesmic Reaction Energies for Reactions 3a and 3b in kcal/mol at the HF/6-31+G* (normal font), B3LYP/6-31+G* (italics), and the MP2(full)/6-31+G* (bold) Levels of Theory

	reaction 3a for **7a**=**E**$^{+\bullet}$			reaction 3b for **7b**=**E**$^{+\bullet}$		
compound	HF	*B3LYP*	**MP2(full)**	HF	*B3LYP*	**MP2(full)**
7a−**b** (E=lp)	2.2	*22.0*	**18.0**	0.6	*24.7*	**26.6**
8a−**b** (E=O)	−7.5	*1.6*	**6.7**	−4.3	*8.1*	**20.5**
9a−**b** (E=S)	−7.9	*2.6*	**11.9**	−7.9	*6.5*	**21.2**
6a−**b** (E=NH)	−5.4	*3.7*	**9.9**	−5.8	*8.6*	**19.8**
5a−**b** (E=CH_2)	−5.0	-	**11.1**	−5.9	-	**21.6**

PN_{ax} distances (weaker transannular bond) obtained for the **5b**−**9b** series. The energy difference between reactions 2b and 1b has a nearly constant energy (ca. 20 kcal/mol) throughout the **5b**−**9b** series. This stabilization energy is in agreement with our above estimation for the stabilization of the short bond radical cations associated with the formation of the transannular bond.

$$\mathbf{7a}{=}E^{+\bullet}\,(\text{short}) + 3\,NH_3 + 3\,CH_4 \rightarrow Et_3N + 3\,MeNH_2 + E{=}P(NH_2)_3^{+\bullet} \quad (2a)$$

$$\mathbf{7b}{=}E^{+\bullet}\,(\text{short}) + 3\,NH_3 + 3\,CH_4 \rightarrow Et_3N + 3\,MeNH_2 + E{=}P(NHMe)_3^{+\bullet} \quad (2b)$$

$$\mathbf{7a}{=}E^{+\bullet}\,(\text{long}) + 3\,NH_3 + 3\,CH_4 \rightarrow Et_3N^{+\bullet} + 3\,MeNH_2 + E{=}P(NH_2)_3 \quad (3a)$$

$$\mathbf{7b}{=}E^{+\bullet}\,(\text{long}) + 3\,NH_3 + 3\,CH_4 \rightarrow Et_3N^{+\bullet} + 3\,MeNH_2 + E{=}P(NHMe)_3 \quad (3b)$$

Cations Obtained by Protonation. Protonation of compounds **7a**=**E** and **7b**=**E** can take place at **E** resulting in **7H**$^+_{(E)}$=**E** (if E: lp at phosphorus), or at the axial nitrogen lone pair resulting in **7H**$^+_{(Nax)}$=**E**. The important structural parameters obtained at the different levels of theory for the **7H**$^+_{(E)}$=**E** series are collected in Table 9. The structural characteristics of the **7H**$^+_{(E)}$=**E** series resemble those of the short bond radical cations. The **7H**$^+_{(Nax)}$=**E** cations wherein protonation took place at the axial nitrogen (see structural data in the Supporting Information, Table S3) are similar to the long bond radical cations, the P−N_{ax} distance being larger than 3.5 Å for these molecules. Likewise in the case of the short bond radical cations for the methylated **5bH**$^+_{(C)}$, **6bH**$^+_{(N)}$, **8bH**$^+_{(O)}$, and **9bH**$^+_{(S)}$, the transannular distance is about 0.5−0.6 Å longer than for the corresponding **5aH**$^+_{(C)}$, **6aH**$^+_{(N)}$, **8aH**$^+_{(O)}$, and **9aH**$^+_{(S)}$ series. The equatorial nitrogens flatten out in case of the methylated series indicating stronger donation of the lone pairs. Available X-ray structures in this series have been obtained for **5bH**$^+_{(C)}$[12] and **6bH**$^+_{(N)}$[34] which also have 2.7−2.8 Å P−N_{ax} distances, in reasonable agreement with the calculated values. Protonation at the axial nitrogen is energetically always less favorable, with the smallest energy difference for the **a** series, being 12.4 kcal/mol (B3LYP/6-31+G*) for **9a**, resulting in a long cation. The energy difference between the two protonated forms of **9b** is even smaller (being about 5 kcal/mol, see Table 11). It is interesting in this regard that it was possible to isolate and characterize the regioisomeric product salts of the reaction of **9b** with MeI and EtI in which the sulfur or the axial nitrogen was alkylated.[37]

Isodesmic reactions were also constructed for the protonated sytems. These reaction energies are related to the stability of the protonated form and are therefore of importance in an understanding of the basicity of the proazaphosphatranes.

$$\mathbf{7a}{=}EH_{(E)}^{+}\,(\text{short}) + 3\,NH_3 + 3\,CH_4 \rightarrow Et_3N + 3\,MeNH_2 + HE{=}P(NH_2)_3^{+} \quad (4a)$$

$$\mathbf{7b}{=}EH_{(E)}^{+}\,(\text{short}) + 3\,NH_3 + 3\,CH_4 \rightarrow Et_3N + 3\,MeNH_2 + HE{=}P(NHMe)_3^{+} \quad (4b)$$

$$\mathbf{7a}{=}EH_{(N)}^{+}\,(\text{long}) + 3\,NH_3 + 3\,CH_4 \rightarrow Et_3NH^{+} + 3\,MeNH_2 + HE{=}P(NH_2)_3 \quad (5a)$$

$$\mathbf{7b}{=}EH_{(N)}^{+}\,(\text{long}) + 3\,NH_3 + 3\,CH_4 \rightarrow Et_3NH^{+} + 3\,MeNH_2 + HE{=}P(NHMe)_3 \quad (5b)$$

Reaction 4a can be used for the short-bonded cations and reaction 5a can be employed for their long-bonded counterparts. In reaction 4a, ca. 20 kcal/mol stabilization is obtained at the B3LYP/6-31+G* level (Table 10), which is similar to the stabilization observed for the short-bonded radical cations in reaction 2. Thus, the formation of the transannular bond results in stabilization of the cation, and an increase of the basicity of the proazaphosphatranes investigated. The destabilization in reaction 5a (Table 11) is somewhat larger than in 1a (Table 4), probably as a result of increased ring strain.

For the methylated series (**7b**=**E**) isodesmic reactions similar to those for the **7a**=**E** series (reactions 4b and 5b, Tables 12 and 13, respectively) can be constructed. The isodesmic reaction energies for the protonated series with a short transannular bond (**5bH**$_{(C)}^+$, **6bH**$_{(N)}^+$ and **9bH**$_{(S)}^+$) are about 10 kcal/mol smaller than the corresponding values for **5aH**$_{(C)}^+$, **6aH**$_{(N)}^+$ and **9aH**$_{(S)}^+$ at the same level of theory, and likewise for the corresponding radical cations. For these molecules the P−N_{ax} distance is considerably longer in case of the **b** series of compounds than for the **a** series, while in contrast, the P−N_{eq} distance simultaneously becomes smaller. The most notable example is **5bH**$_{(C)}^+$, where the B3LYP/6-31+G* structure shows a relatively long P−N_{ax} distance (2.7 Å) in agreement with the X-ray results. By contrast, the HF/6-31G* structure of **5bH**$_{(C)}^+$ reported by Windus et al.[6] has a significantly shorter transannular bond (2.217 Å), similar to that in **5aH**$_{(C)}^+$ (2.262 Å).[6] Apparently, to compensate the electron deficit at phosphorus, there is a competition in donating electron density to the phosphorus occurring between the three equatorial nitrogens and the axial

(37) Tang, J.-S.; Verkade, J. G. *J. Am. Chem. Soc.* **1993**, *115*, 1660−1664.

Table 9. Important Structural Parameters of **7H$^+_{(E)}$=E** Conjugated Acids at the HF/6-31+G* (normal font), B3LYP/6-31+G* (italics), and the MP2(full)/6-31+G* (bold) Levels of Theory[a]

	7aH$^+_{(E)}$=E					**7bH$^+_{(E)}$=E**				
compound	P=E Å	P–N$_{eq}$ Å	P–N$_{ax}$ Å	Σ∠ (N$_{eq}$) deg.	$\Delta E_{S/L}$ kcal/mol	P=E Å	P–N$_{eq}$ Å	P–N$_{ax}$ Å	Σ∠ (N$_{eq}$) deg.	$\Delta E_{S/L}$ kcal/mol
		1.655	2.128	355.7	25.0		1.670	2.073	356.2	29.7
7H$_{(P)}^+$ (E=lp)		*1.682*	*2.137*	*353.8*	*21.6*		*1.699*	*2.104*	*354.4*	*27.1*
		1.677	**2.067**	**353.4**	**28.9**		**1.692**	**2.043**	**352.1**	**33.8**
	1.618	1.652	2.093	356.3	22.9	1.590	1.631	2.669	358.8	14.3
8H$_{(O)}^+$ (E=O)	*1.652*	*1.678*	*2.105*	*354.8*	*21.4*	*1.647*	*1.694*	*2.236*	*353.7*	*13.2*
	1.653	**1.673**	**2.036**	**353.7**	**27.5**	**1.650**	**1.691**	**2.117**	**350.4**	**18.4**
	2.136	1.656	2.151	355.8	10.5	2.098	1.636	2.774	358.9	6.2
9H$_{(S)}^+$ (E=S)	*2.171*	*1.684*	*2.152*	*354.0*	*12.4*	*2.137*	*1.661*	*2.750*	*358.5*	*5.8*
	2.147	**1.678**	**2.068**	**353.7**	**17.4**	**2.115**	**1.657**	**2.524**	**357.0**	**6.7**
	1.681	1.656	2.212	355.3	47.3	1.653	1.637	2.784[b]	358.8	42.9
6H$_{(N)}^+$ (E=NH)	*1.706*	*1.684*	*2.186*	*354.1*	*43.8*	*1.683*	*1.669*	*2.677*[b]	*357.4*	*36.9*
	1.705	**1.679**	**2.088**	**353.9**	**50.6**	**1.690**	**1.676**	2.395[b]	**353.3**	**40.8**
	1.822	1.659	2.288	354.2	67.8	1.817	1.644	2.813[c]	358.8	65.6
5H$_{(C)}^+$ (E=CH$_2$)	*1.842*	*1.688*	*2.236*	*352.8*	*63.6*	*1.836*	*1.670*	*2.773*[c]	*357.9*	*58.3*
	1.829	**1.683**	**2.131**	**352.2**	**70.9**	**1.836**	**1.666**	**2.591b**	**355.9**	**62.2**

[a] $\Delta E_{S/L}$ (in kcal/mol) is the energy difference of the short and long bond structures. [b] The value of 2.859 Å was obtained from the X-ray structure (ref 34). For **7b=NPh** the corresponding value was 2.551(3) Å (Tang, J.; Dopke, J.; Verkade, J. G. *J. Am. Chem Soc*. **1993**, *115*, 5015). This large change shows again the sensitivity of the transannular distance to external effects. [c] The value of 2.773 Å was obtained from the X-ray structure (ref 13).

Table 10. Isodesmic Reaction Energies for Reactions **4a** and **4b** in kcal/mol at the HF/6-31+G* (normal font), B3LYP/6-31+G* (italics) and the MP2(full)/6-31+G* (bold) Levels of Theory

	reaction 4a for **7a=E$^{+\bullet}$**			reaction 4b for **7b=E$^{+\bullet}$**		
compound	HF	*B3LYP*	**MP2(full)**	HF	*B3LYP*	**MP2(full)**
7a−b (E=lp)	23.7	*27.6*	**43.7**	19.4	*26.4*	**49.0**
8a−b (E=O)	22.8	*26.5*	**43.6**	10.4	*15.5*	**41.4**
9a−b (E=S)	20.9	*24.9*	**43.9**	8.4	*11.6*	**36.9**
6a−b (E=NH)	14.3	*18.3*	**34.8**	5.3	*8.5*	**31.6**
5a−b (E=CH$_2$)	16.3	*20.0*	**37.0**	7.5	*10.1*	**33.2**

Table 11. Isodesmic Reaction Energies for Reactions **5a** and **5b** in kcal/mol at the HF/6-31+G* (normal font), B3LYP/6-31+G* (italics), and the MP2(full)/6-31+G* (bold) Levels of Theory

	reaction 5a for **7a=E$^{+\bullet}$**			reaction 5b for **7b=E$^{+\bullet}$**		
compound	HF	*B3LYP*	**MP2(full)**	HF	*B3LYP*	**MP2(full)**
7a−b (E=lp)	0.5	*7.1*	**12.6**	−9.0	*3.6*	**20.9**
8a−b (E=O)	−8.5	*−4.4*	**2.8**	−12.9	*−0.5*	**17.4**
9a−b (E=S)	−8.7	*−3.9*	**7.9**	−16.3	*−2.9*	**18.0**
6a−b (E=NH)	−6.5	*−3.2*	**5.9**	−14.5	*−1.5*	**16.4**
5a−b (E=CH$_2$)	−6.0	*−2.5*	**7.0**	−14.8	*−1.3*	**17.3**

nitrogen as shown in Figure 5, resulting in a fine balance of these two effects. Depending on the level of theory used, one of these effects dominates, and as a very important additional apparent consequence, the transannular distance shows a large dependence on the theoretical method applied. It is worthy to note in this respect that this distance in the MP2/6-31+G* structure of **5bH$_{(C)}^+$** is considerably shorter (by 0.182 Å) than the distance obtained from the X-ray structure (2.773 Å),[13] while the B3LYP/6-31+G* value matches exactly with the solid-state value. Taking into consideration the effect of the condensed phase on polar bonds[22,23] as discussed above, it seems that again MP2 overestimates the transannular bond strength. Despite the 2.773 Å P−N$_{ax}$ distance in **5bH$_{(C)}^+$**, there is still 12−15 kcal/mol stabilization energy (depending on the level of the theory) obtained when subtracting the energies of reactions 4b and 1b. Moreover, the P−N$_{ax}$ distance in **5bH$_{(C)}^+$** shortens by 0.5 Å in comparison with **5b**. Furthermore the P−N$_{eq}$ bond lengths also shorten upon protonation, resulting in an additional stabilization, that contributes to the basicity of **5b**.

The Greater Basicity of 5b Compared with 3. As concluded from the above results, the protonation of **5b** results in extra stabilization with respect to H$_2$C=P(NMe$_2$)$_3$, which can be related to the formation of a weak transannular bond in the former species. Although this bond is weak (as indicated by the large PN$_{ax}$ distance and the decreased isodesmic reaction energy with respect to **5a**, see Table 10), and the electron density at the bond critical point is small, it still contributes to the stability of the protonated form by about 10 kcal/mol (Table 10). As a result, **5b** should be even more basic than **3**, in accordance with previous theoretical predictions.[7]

Comparison of the Basicities of 5b and 7b via ^{31}P NMR Spectroscopy. It is of interest to compare the basicities of **5b** with **7b** in which the basic center in the latter is phosphorus whereas it is the P−C carbon in the former. The reaction of **5b** with [**7bH$^+_{(P)}$**]Cl$^-$ in dry THF was monitored by ^{31}P NMR spectroscopy. The ^{31}P NMR spectrum of the above solution after 12 h displayed complete disappearance of peaks corresponding to **5b** (δ_P 65 ppm) and [**7bH$^+_{(P)}$**]Cl (δ_P −10.6 ppm) and the appearance of new peaks at 48.3 and 120.8 ppm corresponding to **5bH$^+_{(C)}$Cl$^-$** and **7b**, respectively.[13,38,39,40] When **5bH$^+_{(C)}$** was allowed to react with **7b** in THF, no new ^{31}P signals appeared and those for the starting materials remained unchanged. These results indicate that as expected, **5b** is more basic than **7b** and they also agree with the theoretical predictions of Windus et al.[6] and of Schwesinger and co-workers[7] that **5a** is more basic than **7a**.

Attempts to Synthesize 10. To investigate the stabilizing effects in **5bH$^+_{(C)}$**, we attempted to synthesize the bicyclic compound **10**, in which no transannular bond can be formed. The reaction of **11** with MeI in a 1:1 molar ratio in either C$_6$D$_6$ or CD$_3$CN gave rise to a mixture of products along with unreacted **11** according to ^{31}P NMR spectroscopy, rather than the desired salt **12**. This is probably due to alkylation at both the phosphorus and the nitrogen atoms of **11**, a result which is

(38) Lensink, C.; Xi, S. K.; Daniels L. M.; Verkade, J. G. *J. Am. Chem. Soc*. **1989**, *111*, 3478−3479.
(39) Schmidt, H.; Lensink, C.; Xi, S. K.; Verkade, J. G. *Z. Anorg. Allg. Chem.* **1989**, *578*, 75−80.
(40) Tebby, J. C. *Handbook of Phosphorus-31 Nuclear Resonance Data*; CRC Press: Boca Raton, FL, 1991, Chapter 8, p 181.

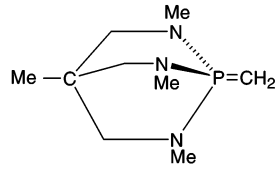

10

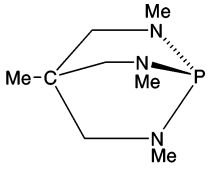

11

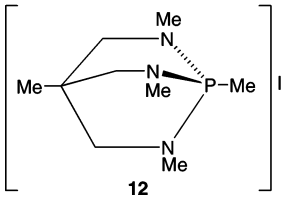

12

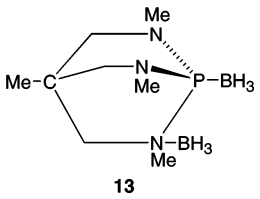

13

not surprising considering the relatively poor σ-basicity of **11** compared with $P(NMe_2)_3$ and with **7b**.[41] Previously, we showed that the reaction of **11** with B_2H_6 in a 1:1 molar ratio gave the di-adduct **13**,[42,43] suggesting that the basicity difference between the phosphorus and nitrogen in **11** is not large. Consequently, we were unable to isolate **12** from the mixtures obtained and hence the synthesis of **10** for comparison studies was thwarted.

Conclusions

The successful synthesis of **5b** allowed the spectroscopic and structural elucidation of the entire **7b=E** series of proazaphosphatranes (**E**: lp, CH_2, NH, O, S) to be realized. By also utilizing the results of quantum chemical calculations at different levels of theory, the following picture has emerged. The calculations carried out at the HF, MP2, and B3LYP levels of theory predict similar structural characteristics, with the exception of the transannular PN_{ax} distance. This structural feature shows a large dependence upon the level of approximation used, and it is also sensitive to the substituent at the equatorial nitrogens. In agreement with the calculated results, the structures of the isolated N_{eq}(alkyl) proazaphosphatranes (**5b**−**9b**) are characterized by the presence of planar equatorial nitrogens, which facilitate effective back-donation of their nitrogen lone pairs toward phosphorus. The planarity of the alkyl-substituted equatorial nitrogens in this series differs from those in the parent molecules (H at N_{eq}) which are more pyramidal and which in addition possess shorter transannular distances than their alkyl derivatives, since weaker back-bonding from the lone pairs of the equatorial nitrogens allows a stronger transannular interaction.

The differences between the parent molecules **7a=E** (**E**: lp, O, S, NH, CH_2) and their N_{eq}(Me) derivatives (**7b=E**) become more striking when, upon protonation or ionization at **E** in **7=EH$^+$$_{(E)}$** and **7=E$^{+\bullet}$**, respectively, the positive charge at phosphorus increases significantly. Thus by simply substituting the hydrogens with methyl groups at N_{eq}, the PN_{ax} distance can increase by as much as 0.5 Å! Upon protonation or ionization of the experimentally isolable **7b=E** series, the strength of the transannular bond as estimated by isodesmic reactions, decreases from 22 to 25 kcal/mol to 12−15 kcal/mol compared with the parent cationic N_{eq}(H) systems. Nevertheless, the formation of the transannular bond contributes to the stabilization of the protonated species while simultaneously increasing the basicity of the proazaphosphatrane bases.

Ylide **5b**, which was predicted from earlier computational studies to be a stronger base than **7b**,[6,7] has been shown by ^{31}P NMR experiments to deprotonate **7bH$^+$$_{(P)}$** quantitatively. This result is in accord with the ionization energy of **5b** which was observed to possess the lowest value (6.3 eV) of the series of compounds we have investigated.

Experimental and Computational Section

All reactions were carried out under argon. Solvents were purified by standard procedures[44] prior to use and **5bH$^+$$_{(C)}$**,[13] **7b**,[39] **7bH$^+$$_{(P)}$**Cl,[38] and **11**[43] were prepared by published methods. High-resolution mass spectral analyses were carried out on a KRATOS MS-50 spectrometer and ^{1}H and ^{13}C{^{1}H} NMR spectra were recorded on a Bruker DRX-400 NMR spectrometer. Phosphorus-31 NMR spectra were recorded on a Bruker DRX-400 NMR spectrometer using 85% H_3PO_4 as the external standard.

Preparation of $N(CH_2CH_2NMe)_3P{=}CH_2$ (5b). Liquid ammonia (120.0 mL) was condensed into a dry ice/acetone-cooled 250 mL round-bottom flask (flask A) that contained sodium (ca. 2.0 g). The flask was connected to another 250 mL round-bottom flask (flask B) by a glass tube. Ammonia was then distilled from flask A into flask B by cooling the latter with a dry ice/acetone mixture. To the distilled ammonia (120 mL) in flask B was added freshly cut sodium (0.6590 g, 28.65 mmol) and the resulting mixture was kept undisturbed for 60 min to allow the sodium to dissolve. Subsequently, **5bH$^+$$_{(C)}$** (2.0474 g, 5.7156 mmol) was introduced into the reaction mixture and the resulting slurry was kept at −78 °C for an additional 1 h. Ammonia was slowly evaporated under a flow of argon while the reaction mixture was stirred. Pentane (150 mL) was added to the residue and the mixture was stirred for 12 h. The pentane-soluble material was cannulated into a Schlenk flask, the volume of pentane was reduced to ca. 20 mL and the flask was cooled to −20 °C for 4 h to obtain colorless crystals of **5b**. The yield of **5b** after crystallization varied from batch to batch in the range of 11.0 to 40.0% (see Discussion). Compound **5b** is highly sensitive to air and moisture and it sublimes readily (80 °C/0.1 mTorr) to give a colorless solid. ^{31}P NMR (C_6D_6): δ_P 64.95 (s). ^{1}H NMR (C_6D_6): δ_H 0.58 (br, 2H, CH_2), 2.48 (t, 6H, $N_{ax}CH_2$, $^3J_{HH}$ = 4.4 Hz), 2.60 (dt, 6H, $N_{eq}CH_2$, $^3J_{PH}$ = 12.0 Hz; $^3J_{PH}$ = 4.4 Hz), 2.76 (d, 9H, NCH_3, $^3J_{HH}$ = 8.8 Hz). ^{13}C NMR (C_6D_6): δ_C −2.37 (d, 1C, CH_2 $^1J_{PC}$ = 366.1 Hz), 36.95 (d, 3C, $N_{eq}CH_2$, $^2J_{PC}$ = 14.3 Hz), 50.57 (s, 3C, NCH_3) 51.92 (s, 3C, $N_{ax}CH_2$). HRMS *m/z* calculated for $C_{16}H_{23}N_4P$: 231.16604. Found 231.166040 (M^+). Attempts to obtain elemental analyses of **5b** were unsuccessful because of the extreme sensitivity of this compound to moisture.

Comparison of the Basicities of 5b and 7b. To a solution of **5b** (12 mg, 50 μmol) in THF (0.40 mL) in a 5 mm NMR tube was added a solution of [**7bH$^+$$_{(P)}$**]Cl (13 mg, 50 μmol) in THF (0.30 mL). The reaction mixture was kept at room temperature with occasional shaking. Phosphorus-31 NMR spectroscopy was used to monitor the reaction. To a solution of **5bH$^+$$_{(C)}$** (18 mg, 50 μmol) in THF (0.40 mL) in a 5 mm NMR tube was added a solution of **7b** (11 mg, 50 μmol) in THF (0.30 mL). The reaction mixture was kept at room temperature with occasional shaking while it was monitored by ^{31}P NMR spectroscopy.

Reaction of 11 with MeI in C_6D_6. Compound **11** (0.11 g, 0.59 mmol) was dissolved in C_6D_6 (1 mL) in a 5 mm NMR tube and then the contents of the tube were cooled to 5 °C. MeI (0.08 g, 0.56 mmol) was syringed into the above solution followed by briefly shaking the tube, which was then left at ambient temperature for 12 h with occasional shaking. This procedure resulted in the formation of a colorless solid. After syringing the supernatant solution out of the NMR tube, the ^{31}P NMR spectrum of the colorless solid was recorded after

(41) Thirupathi, N.; Liu, X.; Verkade, J. G. *Inorg. Chem.* **2003**, *42*, 389−397.
(42) Kroshefsky, R. D.; Verkade, J. G.; Pipal, J. R. *Phosphorus and Sulfur* **1979**, *6*, 377−389.
(43) Laube, B. L.; Bertrand, R. D.; Casedy, G. A.; Compton, R. D.; Verkade, J. G. *Inorg. Chem.* **1967**, *6*, 173−176.
(44) Amerego, W. L. F.; Perrin, D. D. *Purification of Laboratory Chemicals*, 4th ed.; Butterworth and Heinemann: Oxford, 1996.

dissolving it in C_6D_6, revealing peaks at 57.4, 19.0, 18.6 (major), 13.5 and 12.9 (major) ppm. The ^{31}P NMR spectrum of the supernatant revealed the presence of unreacted **11**.

Reaction of 11 with MeI in CD_3CN. Compound **11** (0.19 g, 1.0 mmol) was dissolved in CD_3CN (1 mL) in a 5 mm NMR tube and then the contents of the NMR tube was cooled to 5 °C. MeI (0.14 g, 0.99 mmol) was syringed into the above solution followed by briefly shaking the tube which was then left at the same temperature for 12 h. This resulted in the formation of a colorless solid that was isolated by syringing out the supernatant solution. The ^{31}P NMR spectrum of the solid in CD_3CN revealed peaks at 112.2 (major), 57.7, 19.5 and 13.0 (major) ppm while that of the original supernatant revealed peaks at 112.2 (major), 58.5, 24.0, 19.1, 16.4 along with a peak corresponding to **11**.

X-ray Crystallographic Data Collection and Solution Refinement for 5b. The sample was moisture and air sensitive. A colorless prismatic crystal with approximate dimensions 0.40 × 0.21 × 0.15 mm^3 was selected under ambient conditions, immediately covered with epoxy glue and mounted and centered in the X-ray beam using a video camera at low temperature. Crystal evaluation and data collection were performed at 173 K on a Bruker CCD-1000 diffractometer with Mo K_α ($\lambda = 0.71073$ Å) radiation and a detector to crystal distance of 4.1 cm. The initial cell constants were obtained from three series of ω scans at different starting angles. Each series consisted of 30 frames collected at intervals of 0.3° in a 10° range about ω with an exposure time of 10 s per frame. A total of 43 reflections were obtained. The reflections were successfully indexed by an automated indexing routine built into the SMART program. The final cell constants were calculated from a set of 2882 strong reflections from the actual data collection. The data were collected using a full sphere routine. A total of 25 129 data were harvested by collecting four sets of frames with 0.3° scans in ω with an exposure time of 20 s per frame. This data set was corrected for Lorentz and polarization effects. The absorption correction was based on fitting a function to the empirical transmission surface as sampled by multiple equivalent measurements[44] using SADABS software.[46]

The systematic absences in the diffraction data were consistent for the space group $P2_1/c$ which yielded chemically reasonable and computationally stable results of refinement. The positions of the non-hydrogen atoms were found by direct methods. All remaining atoms including all hydrogens were located in an alternating series of least-squares cycles and difference Fourier maps. All non-hydrogen atoms were refined in a full-matrix anisotropic approximation. All hydrogen atoms were refined in an isotropic approximation. The final least-squares refinement of 455 parameters against 6029 independent reflections converged to R (based on F^2 for $I \geq 2\sigma$) and wR (based on F^2 for $I \geq 2\sigma$) values of 0.032 and 0.083, respectively.

The solution of the crystal and molecular structure of **5b** by X-ray means was carried out at the Iowa State Molecular Structure Laboratory.

Photoelectron Spectra. The He I photoelectron spectra were recorded using an instrument described previously.[47] For calibration of the band positions, methyl iodide, nitrogen, argon and the He^+ peak were used as internal standards. The resolution during the measurements was 40 meV at the $^2P_{3/2}$ Ar line.

Computations. For the quantum chemical calculations, the GAUSSIAN 98 suite of programs[48] was used. Geometry optimizations were carried out at the HF/6-31+G*, B3LYP/6-31+G*, and at the MP2/6-31+G* levels of the theory. The diffuse functions were utilized for a better description of the possible long-range interaction between the axial nitrogen and phosphorus. Second derivatives were calculated at the HF and DFT levels only. None of the optimized structures exhibited negative eigenvalues of the Hessian matrix. Calculation of the radical cations revealed that spin contamination of the wave function was small as judged by the S^2 values which were between 0.75 and 0.77. In the case of the two proazaphosphatrane cationic bond-stretch isomers (**7a**$^{+\bullet}$) CCSD(T)/cc-PVDZ//B3LYP/6-31+G* calculations were also carried out, since the B3LYP and the MP2 results differed considerably. The molecular orbitals were plotted using the MOLDEN program.[30]

Acknowledgment. The authors are grateful to the National Science Foundation and to the Hungarian Research Fund (OTKA Grants T 049258, 034768 and D42216) for grant support of this research. Generous allocation of computer time from the NIIF Supercomputer Center (Budapest) is also gratefully acknowledged.

Supporting Information Available: Total energies and optimized structures for **5a**−**9a**, **5b**−**9b** and their protonated and radical cation forms. This material is available free of charge via the Internet at http://pubs.acs.org.

JA0547533

(45) Blessing, R. H. *Acta Cryst*. 1995, *A51*, 33−38.
(46) All software and sources of the scattering factors are contained in the SHELXTL (version 5.1) program library (G. Sheldrick, Bruker Analytical X-ray Systems, Madison, WI).
(47) Veszprémi, T.; Zsombok, Gy. *Magy. Kém. Foly*. **1986**, *92*, 39−40.
(48) *Gaussian 98*, revision A.6; Gaussian,Inc.: Pittsburgh, PA, 1998.